Deliver via: PDF EMAIL adrian@wsu.edu 8/29/2003

Adrian Rodriguez-Marek
Washington State University
Civil Engineering
PO Box 642910
Pullman, WA 99164-2910
(509) 335-7088

UW Affiliation: Non-UW
Payment Method: Deposit Account
Bu[35;1H[K[36;1H[Kdget Number/Account Info: 004569 wsu program

Not Wanted After: Sept. 30, 2003
Will Pay Copyright Fee: No
Use Sources Outside HSLIC: No
Rush: *YES*

Citation Information:

Youngs, R. R., and Coppersmith, K. J. (1985). "Implications of fault slip rates and earthqauke recurence models to probabilistic seismic hazard assessments,"

source: Bulletin of the Seismological Society of America

Volume 75, No. 4, pages 939-964

RUSH CHARGES

Bulletin of the Seismological Society of America, Vol. 75, No. 4, pp. 939–964, August 1985

IMPLICATIONS OF FAULT SLIP RATES AND EARTHQUAKE RECURRENCE MODELS TO PROBABILISTIC SEISMIC HAZARD ESTIMATES

By Robert R. Youngs and Kevin J. Coppersmith

Abstract

Increasingly, fault slip rates are being used to constrain earthquake recurrence relationships for site-specific probabilistic seismic hazard (ground motion) assessments. This paper shows the sensitivity of seismic hazard assessments to variations in recurrence models and parameters that incorporate fault slip rates. Two models are considered to describe the partitioning of the slip rate or seismic moment rate into various magnitude earthquakes: an exponential magnitude distribution and a characteristic earthquake distribution. Assuming an exponential distribution, the activity rate, $N(m^o)$, is constrained by the upper bound magnitude, m^u, the *b*-value for the region and the fault slip rate, *S*. For a given *S*, variations in m^u and *b*-value have significant effects on recurrence and computed hazard, depending on whether the assumption is made that the seismicity rate is constant or the moment rate is constant.

There is increasing evidence that the characteristic earthquake model is more appropriate for individual faults than the exponential magnitude distribution. Based on seismicity data from areas having repeated large earthquakes, a generalized recurrence density function is developed, and the resulting recurrence relationship requires only m^u, *b*-value, and *S*. A comparison of the recurrence relationships from this model with the historical seismicity and paleoseismicity data on the Wasatch and San Andreas faults shows a good match. The computed hazard based on the characteristic earthquake model differs from that obtained for the exponential model as a function of the fault-to-site distance and the acceleration level. One check on the recurrence models using slip rate is to compare over large regions activity rates based on seismicity data and slip rate data. Such a comparison in the western Transverse Ranges shows a reasonable match for both the exponential and characteristic earthquake models in the moderate-to-large magnitude range.

Introduction

Probabilistic seismic hazard analyses result in estimates of the probability of exceeding various levels of ground motion by considering earthquake location, timing, and size. Unlike deterministic analyses that only consider ground motions due to the "maximum credible" earthquake, probabilistic analyses are based on the likelihood of occurrence of various magnitude earthquakes and their contributions to ground motion hazards. Therefore, the frequency of earthquake occurrence, or recurrence, is an essential parameter. Increasingly, late-Quaternary fault slip rates are being used to constrain earthquake recurrence relationships for probabilistic seismic hazard assessments. The purpose of this paper is to illustrate the use of fault slip rates to estimate earthquake recurrence and to show the sensitivity of calculated seismic hazard estimates to various assumptions regarding fault-specific seismicity parameters and earthquake recurrence models.

Seismic hazard analyses for engineering purposes are usually conducted for particular sites, rather than regions. Because of this, there has been a move to make hazard assessments as site-specific and as fault-specific as possible. This requires that each fault be characterized by its own earthquake recurrence behavior. Further,

depending on the engineering structure of interest, hazard estimates are usually made for a relatively short future time window (e.g., 50 yr) and for low probability levels (e.g., 10^{-2} to 10^{-4}). The historical seismicity record in the United States and most other areas of the world is generally too short to characterize the recurrence characteristics of particular faults, especially for "rare" or low probability events. To accomplish this, geologic data must be considered.

Fault Slip Rate and Seismic Moment

Geologic data are commonly used to estimate maximum earthquake magnitudes on faults and are becoming increasingly useful in constraining fault-specific earthquake recurrence. Empirical relationships between fault behavior characteristics and magnitude have been compiled for historical earthquakes (e.g., Slemmons, 1977, 1982), and these provide a basis for estimating upper bound magnitudes (e.g., Schwartz *et al.*, 1984). Geologic studies along fault zones such as the San Andreas fault (Sieh, 1978, 1984) and the Wasatch fault, Utah (Swan *et al.*, 1980; Schwartz and Coppersmith, 1984) have been successful at identifying prehistoric earthquakes in the geologic record and at estimating average recurrence intervals between surface-faulting earthquakes. However, this type of paleoseismicity data is usually not available for most faults, even for the most active faults of the San Andreas system. In these cases, the geologic slip rate often proves to be the only available data constraint on earthquake recurrence.

Fault slip rates offer the advantage over historical seismicity data of spanning several seismic cycles of large-magnitude earthquakes on a fault and thus allowing estimates of the average earthquake frequency. However, several assumptions are required: (1) all slip measured across the fault is usually assumed to be seismic slip unless fault creep has been recognized; (2) the slip rate is an average and does not allow for short-term fluctuations in rate to be recognized; (3) the average slip rate is assumed to be applicable to the future time period of interest; and (4) surface measurements of slip rate, which are usually point estimates, are assumed to be representative of slip rates at seismogenic depths and along the length of the fault.

The first and probably the simplest use of slip rate to estimate earthquake recurrence was proposed by Wallace (1970)

$$R = D/S \tag{1}$$

where R is the recurrence interval, D is the displacement per event, and S is the average seismic slip rate (total slip rate minus creep rate). Displacement per event is estimated from past historical earthquakes or from geologic evidence of prehistoric events. A basic assumption of this simple model is that all of the slip along a fault is released by displacement events of size D. No allowance is made for the occurrence of events of various other sizes along the fault.

A more complete approach to the assessment of earthquake recurrence using slip rate is through the use of seismic moment. Seismic moment, M_0, is the most physically meaningful way to describe the size of an earthquake in terms of static fault parameters

$$M_0 = \mu A_r D \tag{2}$$

where μ is the rigidity or shear modulus (usually taken to be $\sim 3 \times 10^{11}$ dyne/cm^2), A_r is the rupture area on the fault plane undergoing slip during the earthquake, and

D is the average displacement over the slip surface (Aki, 1966). The total seismic moment rate $\dot{M}_0^T$ or the rate of seismic energy release along a fault is estimated by Brune (1968)

$$\dot{M}_0^T = \mu A_f S \tag{3}$$

where S is the average slip rate along the fault, and A_f is the total fault plane area. The seismic moment rate provides an important link between geologic and seismicity data. For example, seismic moment rates determined from fault slip rates in a region may be directly compared with seismic moment rates based on seismicity data (e.g., Doser and Smith, 1982). Seismic moment is translated to earthquake magnitude according to an expression of the form

$$\log M_0 = cm + d. \tag{4}$$

In California, Hanks and Kanamori (1979) have indicated $c = 1.5$ and $d = 16.1$ on the basis of both theoretical considerations and empirical observations. The moment magnitude, m, defined in equation (4) is considered to be equivalent to local magnitude in the magnitude range $3 < M_L < 7$ and surface wave magnitude in the magnitude range $5 < M_S < 7\frac{1}{2}$.

Once the fault slip rate is used to constrain the seismic moment rate on the fault, a model must be assumed for the manner in which the rate of moment release is distributed to earthquakes of various magnitudes. Two models are considered in this paper: (1) an exponential distribution of magnitudes; and (2) a distribution appropriate to the characteristic earthquake model.

Anderson and Luco (1983) present the sensitivity of slip rate constrained recurrence relationships to variations in some of the input parameters. Our intent in this paper is to extend these comparisons to examine the sensitivity of *seismic hazard* (probabilistic ground motions) assessments to changes in recurrence parameters, as well as to examine the effects based on both an exponential magnitude distribution model and a characteristic earthquake distribution model.

Exponential Magnitude Distribution

Form of recurrence relationship. The general form of the Gutenberg-Richter (1954) exponential frequency magnitude relationship is (Richter, 1958)

$$\log N(m) = a - bm \tag{5}$$

where $N(m)$ is the cumulative number of earthquakes of magnitude greater than m, and a and b are constants. Equation (5) can be written in the complimentary cumulative form of a shifted exponential distribution as

$$N(m) = N(m^0)\exp(-\beta(m - m^0)) \tag{6}$$

where m^0 is some arbitrary reference magnitude and $\beta = b \cdot \ln 10$.

When applying equations (5) and (6) to an individual fault, or finite volume of crust encompassing a set of faults, the existence of an upper limit to the size of earthquakes that can occur must be introduced, requiring truncation of the magnitude distribution. The most reasonable approach for truncating a distribution is to truncate and renormalize the density function, unless there are compelling argu-

ments to do otherwise (an alternate form of truncation, the characteristic earthquake model, is discussed later in this paper).

The frequency density function for magnitude is obtained by differentiating the complement to equation (6).

$$n(m) = d(N(m^0)(1 - \exp(-\beta(m - m^0))))/dm = N(m^0)\beta\exp(-\beta(m - m^0)). \quad (7)$$

Introducing an upper bound magnitude, m^u, and setting $n(m) = 0$ for $m > m^u$, the truncated density function is renormalized as

$$n(m) = \frac{N(m^0)\beta\exp(-\beta(m - m^0))}{1 - \exp(-\beta(m^u - m^0))} \quad \text{for} \quad m \leqq m^u. \quad (8)$$

Integrating equation (8), the truncated form of equation (6) becomes

$$N(m) = N(m^0)\frac{\exp(-\beta(m - m^0)) - \exp(-\beta(m^u - m^0))}{1 - \exp(-\beta(m^u - m^0))} \quad \text{for} \quad m \leqq m^u. \quad (9)$$

This form was first proposed by Cornell and Van Marke (1969) motivated by the arguments given above. Berrill and Davis (1980) have shown that equation (9) arises naturally from maximum entropy considerations when an upper bound magnitude is assumed to exist.

Other forms of truncation at the upper bound magnitude have been proposed, including generalized forms of the magnitude density function (e.g., Yegulalp and Kuo, 1974; Caputo, 1977; Main and Burton, 1981), quadratic forms of equation (5) (e.g., Shlien and Toksöz, 1970; Merz and Cornell, 1973), and multilinear forms of equation (5). While these forms will not be pursued here, they could readily be used to formulate slip rate constraints on earthquake recurrence.

Slip rate constraints on exponential magnitude recurrence relationships. Several authors (e.g., Smith, 1976; Campbell, 1977; Molnar, 1979; Anderson, 1979; Papastamatiou, 1980) have developed relationships between earthquake recurrence parameters and fault or crustal deformation rates, assuming an exponential magnitude distribution. Anderson and Luco (1983) have reviewed various forms of recurrence relationships that have been developed using slip rate constraints and discuss the use of these constraints in estimating earthquake recurrence parameters.

The link between fault slip rate and earthquake recurrence rates is made through the use of seismic moment. The total rate of seismic moment can be related to earthquake occurrence rate by the expression

$$\dot{M}_0^T = \int_{-\infty}^{m^u} \dot{n}(m)\boldsymbol{M}_0(m)\, dm \quad (10)$$

where $\dot{n}(m)$ is the density function for earthquake occurrence rate [$\dot{n}(m)$ and $\dot{N}(m)$ represent $n(m)$ and $N(m)$ normalized to number of events per unit time]. Using equations (3), (4), and (5), equation (10) can be written as

$$\mu A_f S = b\dot{N}(m^0)M_0^u\exp(-\beta(m^u - m^0))/(c - b)(1 - \exp(-\beta(m^u - m^0))) \quad (11)$$

which is equivalent to the relationship developed by Anderson (1979) and the type 2 relationship presented by Anderson and Luco (1983). The term M_0^u is the moment

for the upper bound magnitude m^u. If uncertainty in the conversion from magnitude to moment, equation (4), is included explicitly, then M_0^u should be replaced by its expected value $E[M_0 \mid m^u]$. Assuming the slip rate, S, on a fault is known, equation (11) provides a constraint on the three parameters of the recurrence relationship $\dot{N}(m^0)$, b, and m^u.

The constraint imposed by fault slip rate allows the development of fault-specific recurrence relationships in regions where the historical seismicity data are only sufficient to establish the regional recurrence rate for small-to-moderate size earthquakes. For each fault in the region, estimates of the upper bound magnitude, m^u, can be made using fault characteristics (e.g., Slemmons, 1982; Schwartz *et al.*, 1984). The historical seismicity data can be used to determine a regional b-value. Assuming the individual faults all have a b-value equal to the regional b-value, the earthquake activity rate for each fault, $\dot{N}(m^0)$, can be computed from the estimated slip rate for the fault using equation (11). Finally, by summing the recurrence relationships developed for the individual faults in the region, an estimate of the overall regional seismicity rate for small-to-moderate earthquakes is obtained. This estimate can be compared with the observed historical seismicity for consistency. Examples of this type of comparison are made later in this paper.

In well-instrumented, seismically active regions, it may be possible to estimate the recurrence rates for small-to-moderate magnitude earthquakes on an individual fault directly from the seismicity catalog. Given values of $\dot{N}(m^0)$ and b-value from historical seismicity, and estimates of the fault slip rate, equation (11) can be used to estimate the upper bound magnitude. Alternatively, if the upper bound magnitude can also be constrained by physical fault characteristics, the slip rate estimates can be used to evaluate the validity of the exponential magnitude distribution versus other recurrence models.

Effect of parameter uncertainty on recurrence relationships and computed seismic hazard. Anderson and Luco (1983) present the sensitivity of slip rate constant recurrence relationships to variations in some of the parameters. Our intent here is to extend these comparisons to examine the sensitivity of hazard assessments to changes in recurrence parameters, in a similar fashion as recently presented by Bender (1983).

The most common formulation used for seismic hazard analysis is that developed by Cornell (1968) is which the occurrence of peak values of a ground motion parameter Z in excess of some specified level, z, are modeled as a Poisson process. The annual probability that the specified ground motion level will be exceeded, $P(Z > z)$, is given by the expression

$$P(Z > z) = 1 - e^{-\nu(z)} \simeq \nu(z) \quad \text{for} \quad \nu(z) \ll 1. \quad (12)$$

The parameter $\nu(z)$ represents the mean annual rate of exceedance of ground motion level z at the site due to the occurrence of earthquakes on all sources that may affect the site. If we restrict our attention to the hazard due to a single source (fault), then $\nu(z)$ is given by

$$\nu(z) = \int_{m^0}^{m^u} \dot{n}(m)P(Z > z \mid m)\, dm. \quad (13)$$

The term $P(Z > z \mid m)$ is the conditional probability that an earthquake of magnitude m occurring on the fault will result in an exceedance, and is a function of the

distribution of distances from the site to earthquakes on the fault and the attenuation of seismic energy from the source to the site. The lower magnitude level m^0 represents the minimum magnitude considered capable of producing ground motions of engineering significance. In practice, the integral in equation (13) is usually replaced by the summation

$$\nu(z) = \sum_i \lambda(m_i) P(Z > z \mid m_i) \tag{14}$$

where $\lambda(m_i)$ is obtained by discretizing the cumulative recurrence relationship, $N(m)$, over the magnitude range m^0 to m^u using an increment Δm.

The use of slip (moment) rate to impose a constraint on the recurrence relationship results in different sensitivity in computed hazard levels to parameter changes than are observed when the recurrence relationships are based solely on historical seismicity. These effects are illustrated using the hypothetical example shown in Figure 1 of three sites located at varying distances from the center of a long fault. The sensitivity in the hazard assessments at these sites is examined for two cases: (1) the annual number of earthquakes occurring on the fault of magnitude $\geqq 4$ is held constant [i.e., $N(m^0)$ equal to a constant based on historical seismicity]; and (2) the rate of seismic moment release is held constant [i.e., $\dot{M}_0^T$ equals a constant based on slip rate].

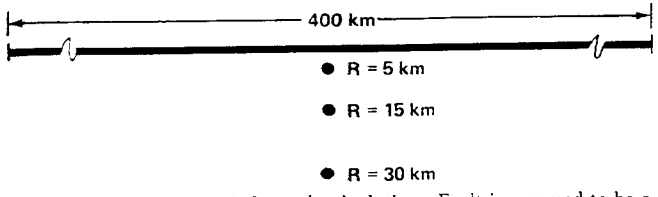

FIG. 1. Hypothetical model for seismic hazard calculations. Fault is assumed to be a vertical strike-slip fault having length of 400 km and down-dip width of 10 km. Example sites are located at distances of 5, 15, and 30 km.

The attenuation relationships used in the examples are those presented by Sadigh (1983), which yield similar estimates of median peak ground acceleration to those obtained using the relationships developed by Campbell (1981) and Joyner and Boore (1981).

The most uncertain parameter in the recurrence relationship for a fault is the overall level of seismic activity (either expressed as the rate above a threshold magnitude or as seismic moment rate). Examining equation (14) indicates that hazard assessments are directly proportional to the overall seismicity rate either expressed directly as the cumulative seismicity rate, $N(m^0)$ [equation (9)], or indirectly through slip rate [equation (11)]. Thus, an increase in seismicity rate translates directly into an equal increase in the rate of exceedance.

The upper bound magnitude for the fault is likely to be the next most uncertain parameter in the recurrence relationship. Figure 2 shows the effect of varying m^u in the range of 6 to 8 in terms of the recurrence relationship for the fault. In this figure, and in many that follow, two analysis cases are considered. In the first, the seismicity rate in terms of the annual number of earthquakes above a particular magnitude (in this case, magnitude 4) is assumed to be constant. This might be appropriate, for example, if the number of earthquakes in the historical seismicity

record is assumed to be a constraint on the activity rate. In the second case, the moment rate is assumed to be constant. This would be appropriate if the fault slip rate is the principle constraint on the activity rate.

For the case of a constant seismicity rate, increasing in the upper bound magnitude results in an imperceptible reduction of the recurrence rate for smaller magnitude events as the number of larger events added represents only a very small fraction of the total number of earthquakes. For the case of a constant moment rate, increasing the upper bound magnitude from 6 to 8 results in a dramatic decrease in the recurrence rate for smaller events, because a single large earthquake contains the equivalent moment of many smaller events.

Figure 3 shows the effect of variations in the upper bound magnitude on the computed hazard at the three sites in Figure 1. Shown are the annual rates of exceeding various levels of peak ground acceleration (generally termed hazard

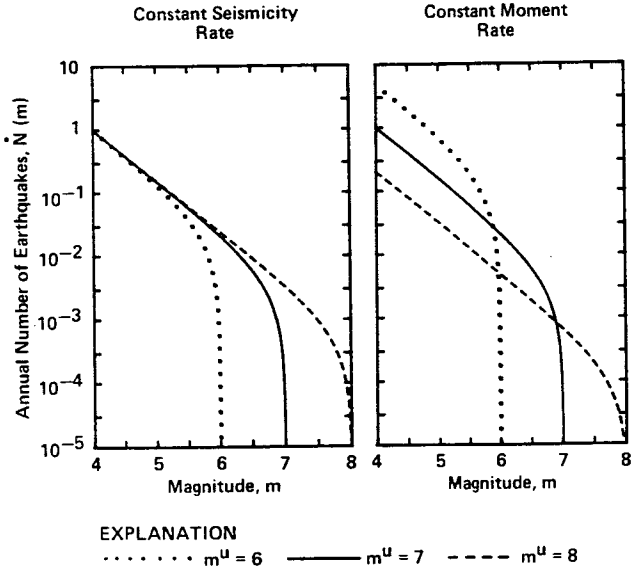

FIG. 2. Effect on the recurrence relationship for a fault of variations in upper bound magnitude, which ranges from 6 to 8 (b-value = 0.8).

curves) obtained using the recurrence curves shown in Figure 2. As can be seen from the top row of plots for the case of a constant seismicity rate, increasing the upper bound magnitude results in an increase in the probability of exceedance, with the effect being more pronounced at larger accelerations and greater distances from the fault. However, for the case of a constant moment rate, increasing the upper bound magnitude results in a decrease in the hazard for sites near the fault, while for larger accelerations and sites at greater distances from the fault, the hazard increases with increasing upper bound magnitude. At various acceleration levels, depending upon the distance to the fault, one observes that the hazard levels at first increase and then decrease as the upper bound magnitude is increased.

The explanation for the effects shown in Figure 3 can be seen by examining the relative contribution of various magnitude earthquakes to the hazard at the three sites. Figure 4 shows the contributions of various magnitudes to hazard as a function

of acceleration level and distance from the fault (for $b = 0.8$ and $m^u = 8$). For the site close to the fault and low to moderate acceleration levels, small to moderate earthquakes contribute the most to the hazard. For the case of a constant seismicity rate, the recurrence rate for the smaller events is relatively unaffected by changes in upper bound magnitude, and thus the hazard curves are also relatively insensitive to changes in upper bound magnitude. For the case of constant moment rate, the recurrence rates for smaller events decrease rapidly as the upper bound magnitude increases (Figure 2), and thus the hazard is reduced.

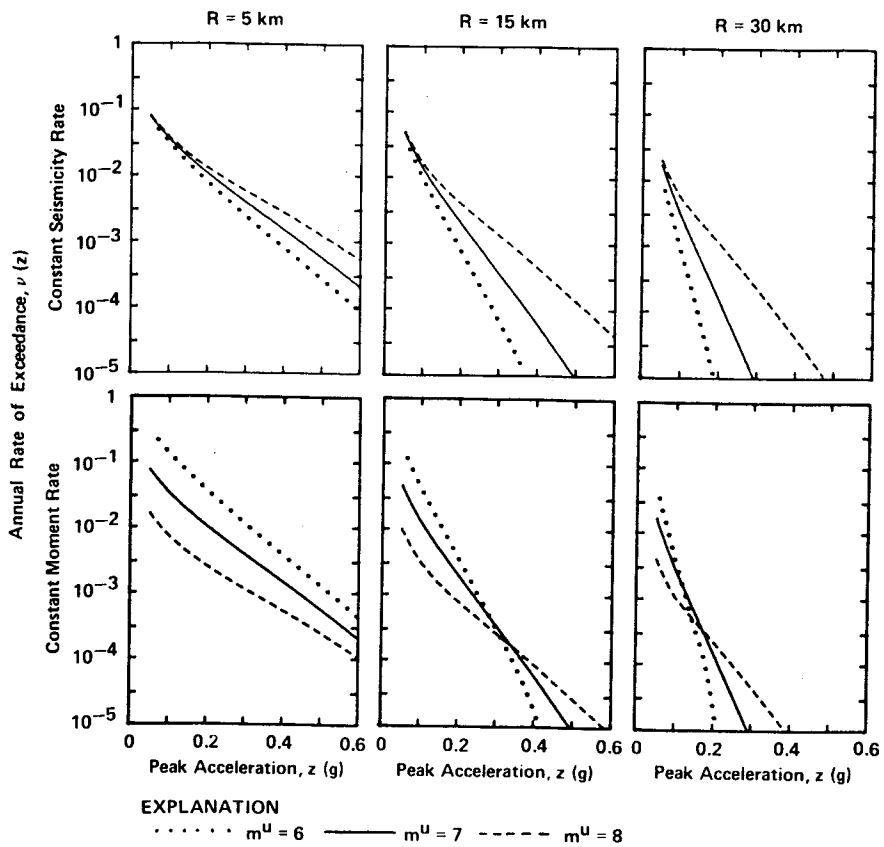

FIG. 3. Effect on computed hazard (peak acceleration) from variations in upper bound magnitude, which ranges from 6 to 8 (b-value = 0.8).

At greater distances from the fault, larger magnitude events become the predominant contributors to hazard, especially at higher acceleration levels. For the case of a constant seismicity rate, including larger events by increasing of the upper bound magnitude continually increases the hazard because the recurrence rate for smaller events remains nearly constant and the larger events are much more likely to produce larger ground motions at the site. For the case of a constant slip rate, there is a trade-off between the larger ground motions produced by the larger magnitude earthquakes and the effect of including these larger events on the

recurrence rates of smaller events. At first, including larger magnitude events increases the hazard, although the effect is not as great as for the case of a constant seismicity rate because the inclusion of larger events reduces the recurrence rate for smaller events. However, once the upper bound magnitude goes beyond the peak of the distributions shown in Figure 4, then the effect of including larger events is to reduce the hazard by reducing the recurrence rate for those events contributing the most to hazard.

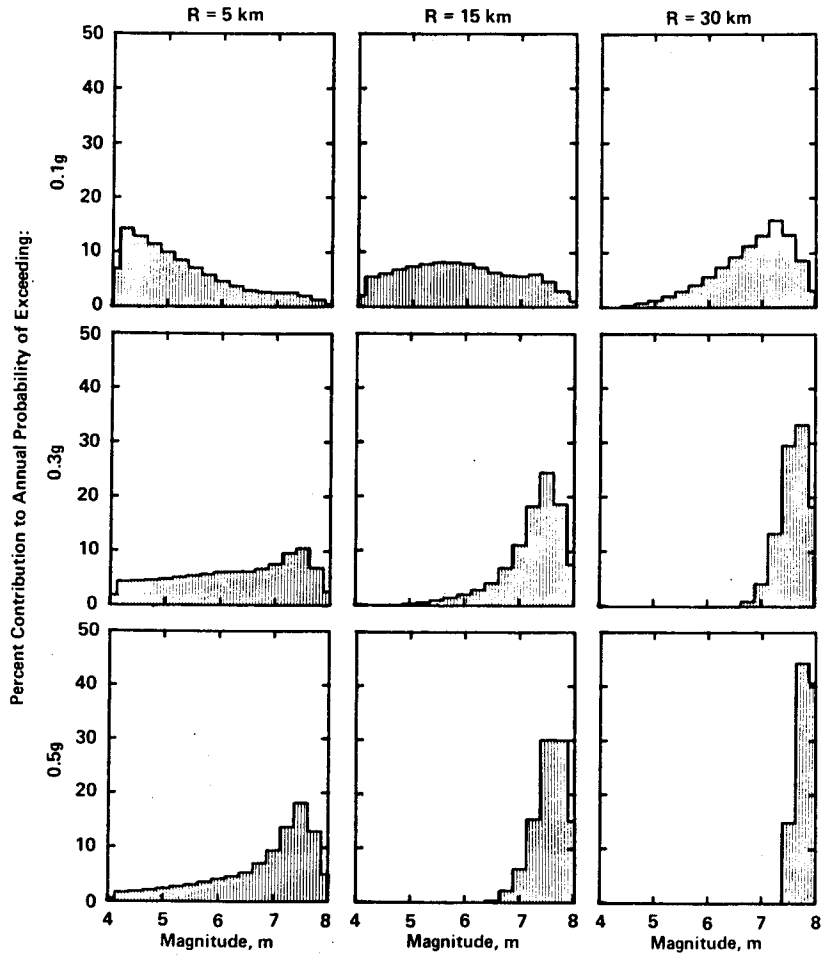

FIG. 4. Relative contribution of various magnitude earthquakes to computed seismic hazard as a function of acceleration and distance from the fault ($b = 0.8$, $m^u = 8$).

The remaining parameter in the recurrence relationship is the b-value. The b-value controls the relative frequency of different magnitude earthquakes, with lower b-values (in absolute value) resulting in an increase in the relative frequency of large events as compared to small events. Studies by Bender (1983) have shown that hazard assessments are sensitive to changes in b-values. However, as was the case for variations in upper bound magnitude, the effect on hazard due to changes

in b-value is different for the case of a constant seismicity rate than for a constant moment rate. Figure 5 shows the effect of changes in b-value in the range of 0.4 to 1.2 on recurrence relationships. For the case of a constant seismicity rate, the recurrence curves are anchored at the minimum magnitude, and changes in the b-value have the greatest effect on the frequency of the larger events. For the case of a constant moment rate, the recurrence curves are anchored at the large magnitudes, and the b-value has the greatest effect on the frequency of the smaller events.

Figure 6 shows the effect of changes in b-value on the computed hazard at the three sites (for $m^u = 7$). At close distances to the fault, changes in b-value assuming a constant seismicity rate has the opposite effect on the hazard than when assuming a constant moment rate. Reducing the b-value increases the computed hazard for the case of a constant seismicity rate and decreases the hazard for the case of constant moment rate. At greater distances from the fault and larger accelerations,

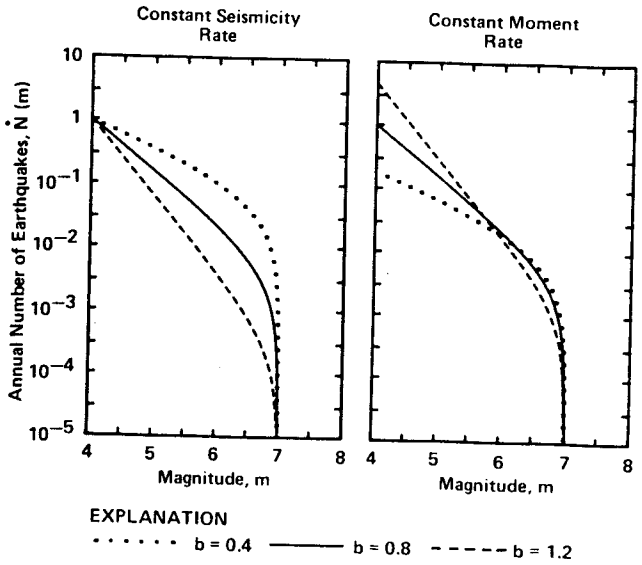

FIG. 5. Effect on recurrence relationships for a fault of variations in b-value, which ranges from 0.4 to 1.2 ($m^u = 7$).

reducing the b-value increases the hazard with the increase much more significant for the case of constant seismicity rate. Again, these results can be readily explained by examining the effect of changes in b-value on the recurrence curves (Figure 5) and the relative contributions of different magnitude earthquakes to hazard as a function of distance and acceleration level (Figure 4). At larger distances and higher acceleration levels, the hazard results primarily from the larger magnitude events. For a constant seismicity rate, changes in b-value have a large effect on the recurrence rate for these events and thus have a large effect on hazard. For a constant moment rate, changes in b-value have little effect on the recurrence rate for larger events and thus have little effect on the computed hazard.

It should be noted that, in practice, when recurrence parameters are obtained from seismicity data, the $N(m^0)$ and b-value estimates are usually coupled such that when the b-value is increased, there is a corresponding increase in $N(m^0)$, producing compensating effects on the computed hazard.

The above comparisons were made for the annual probability of exceeding various levels of peak ground acceleration. If one were considering a ground motion parameter more sensitive to earthquake magnitude, such as peak velocity or spectral acceleration at periods greater than 0.1 sec, or considering the effects on hazards sensitive to ground motion duration, such as liquefaction, then somewhat different sensitivities to parameter variations would be observed. For these ground motion parameters, the contributions from the larger magnitude earthquakes dominate the hazard, and the results are most sensitive to changes in the frequency of these

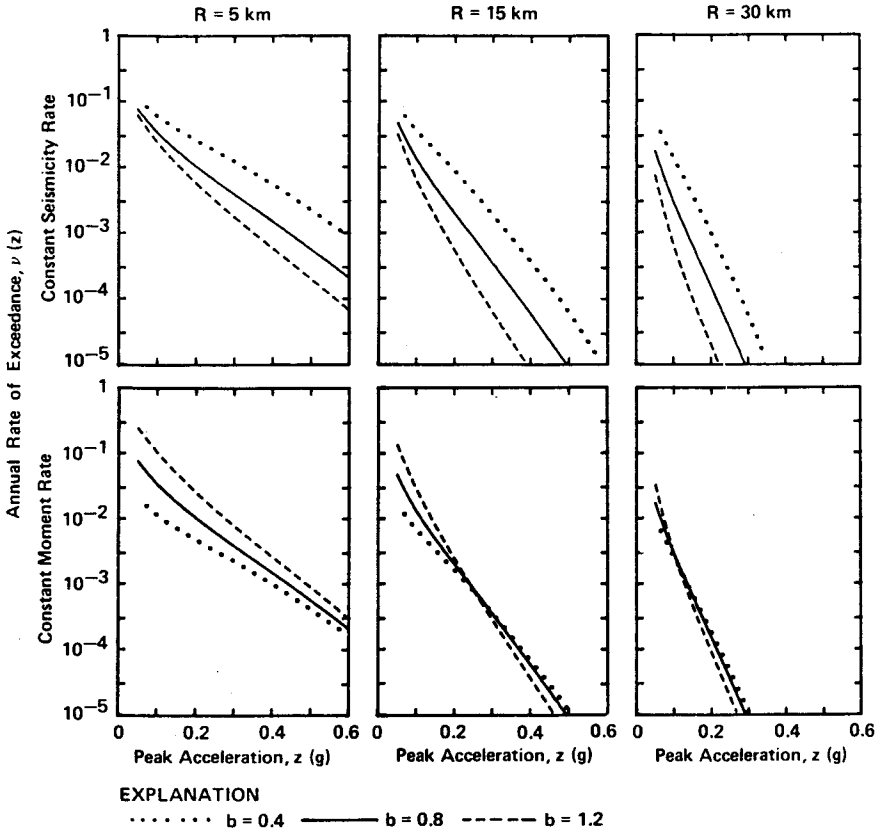

FIG. 6. Effect on computed hazard (peak acceleration) of variations in b-value, which ranges from 0.4 to 1.2 ($m^u = 7$).

events. An example is presented in Figure 7 which shows the effect of variations in upper-bound magnitudes on the annual probability of exceeding various levels of 5 per cent damped spectral acceleration at a period of 1 sec. [The attenuation relationship used is presented in Sadigh (1983)]. Comparison of these results with those shown in Figure 3 show an increased sensitivity to changes in upper bound magnitude for the case of constant seismicity rates. For the case of constant moment rate, the results in Figure 7 show that the point at which an increase in upper bound magnitude produces an increase in hazard occurs at closer distances and lower ground motion levels when longer period ground motions are considered.

Characteristic Earthquake Model

Form of recurrence relationship. Although the distribution of earthquake magnitudes on a seismic source is usually assumed to follow an exponential distribution, there is increasing evidence that a characteristic earthquake model may be more appropriate for individual faults. The characteristic earthquake model (Schwartz and Coppersmith, 1984) is based on the hypothesis that *individual* faults and fault segments tend to generate same-size or characteristic earthquakes. "Same-size" means within about one-half magnitude unit. Characteristic earthquakes occur on

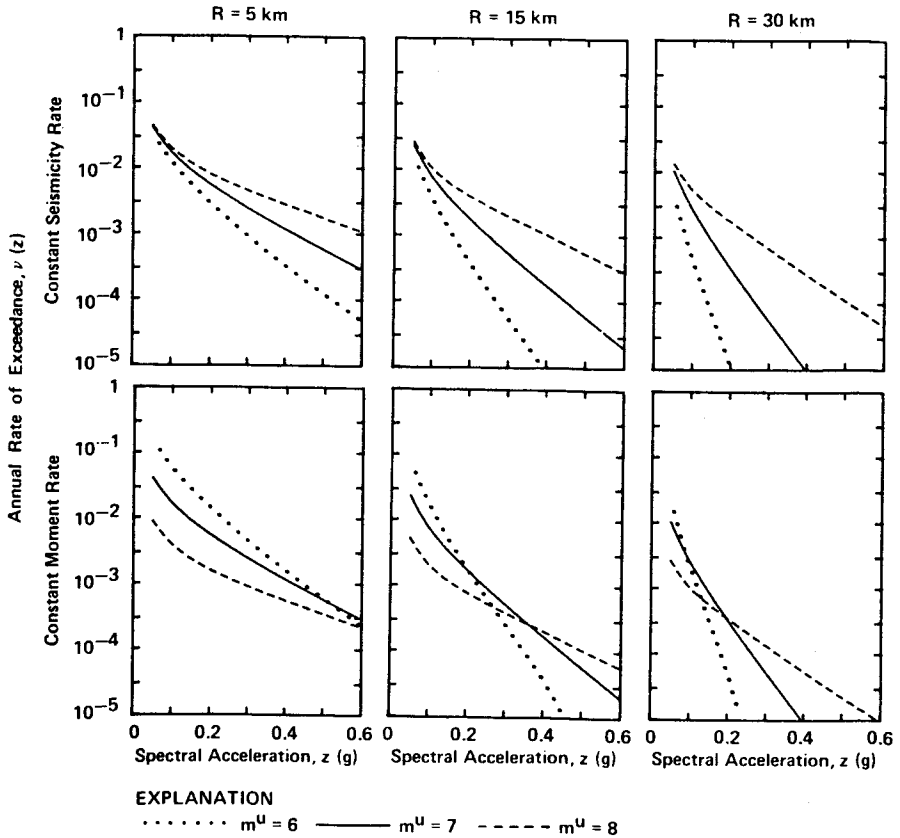

FIG. 7. Effect of variations in upper bound magnitude on annual probability of exceeding various levels of 5 per cent damped spectral acceleration at a period of 1 sec (b-value = 0.8).

a fault not at the exclusion of all other magnitudes, but with a frequency distribution that differs from an exponential magnitude distribution model.

The basis for the characteristic earthquake model lies in both geologic and seismicity data. Geologic investigations along the Wasatch and San Andreas faults indicate repeated same-size displacements associated with paleo-earthquakes along the same segments of the faults (Schwartz and Coppersmith, 1984). This constancy in dimension and displacement strongly suggests constancy in seismic moment or earthquake size. Aki (1984) has suggested that the characteristic earthquake is the

result of the persistence of barriers to rupture through repeated seismic cycles. Bakun and McEvilly (1984) argue for the existence of a characteristic earthquake along the central segment of the San Andreas fault on the basis of nearly identical source parameters for five historical earthquakes.

When geologically derived recurrence intervals for characteristic earthquakes are compared with relationships derived from seismicity data, a marked mismatch occurs (Schwartz and Coppersmith, 1984; Figures 13 and 14). Only by assuming a low b-value in the moderate magnitude range can the geologic data be reconciled with the seismicity data (Figure 8). It should be emphasized that the characteristic earthquake model appears to be applicable to individual faults and fault segments. Large regions, which typically contain a number of faults, usually display exponential recurrence behavior. However, if a seismic hazard analysis is intended to have fault-specific seismic sources, then it may be most appropriate to model the recurrence behavior based on the characteristic earthquake model.

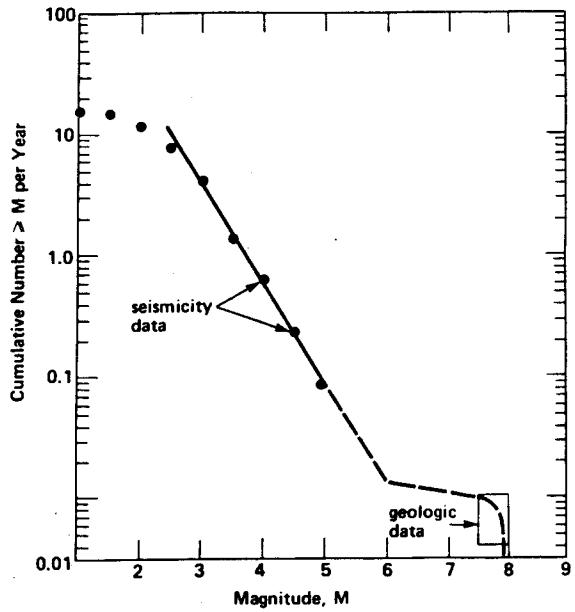

FIG. 8. Hypothetical recurrence relationship for a fault showing the constraints provided by seismicity data and geologic data (modified from Schwartz and Coppersmith, 1984).

In order to observe this type of "nonlinear" recurrence behavior along a particular fault, either geologic data regarding prehistoric earthquake recurrence must be available or an historical seismicity record long enough to include characteristic events is required. In addition, the spatial extent of earthquakes included in the catalog should be restricted enough such that the catalog is dominated by the behavior of an individual fault. In highly active regions containing a large number of faults, the larger the region considered becomes, the less evident is the behavior of any single fault.

In regions where repeated characteristic earthquakes have occurred during historical time, several authors have reported that the seismicity data show the

distinctly nonlinear recurrence relationships predicted by this model (Figure 9). Examples include subduction zones in Alaska (Utsu 1971; Purcaru, 1975; Lahr and Stephens, 1982; Davison and Scholz, 1984) and Mexico (Singh *et al.*, 1981, 1983), and crustal faults in Turkey, Sweden and Greece (Båth, 1981, 1982, 1983), Japan (Wesnousky *et al.*, 1983), and the New Madrid region of the Central United States (Main and Burton, 1984). Note that the recurrence data shown in Figure 9 are reproduced directly from the original publications. These observational data suggest

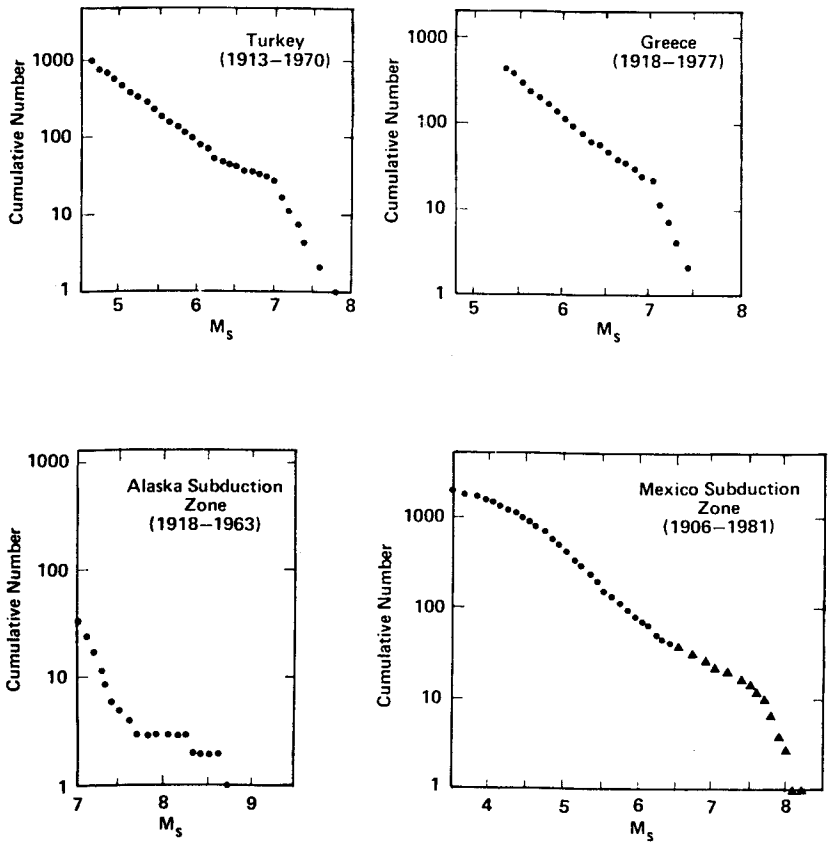

FIG. 9. Frequency magnitude plots based on historical and instrumental seismicity in the Alaska subduction zone (Utsu, 1971), the Mexican subduction zone (Singh *et al.*, 1983), Greece (Båth, 1983), and Turkey (Båth, 1981). On the plot for the Mexican subduction zone, the triangles represent data for the period 1906 to 1981 (75.5 yr); the circles are data from 1963 to 1981 normalized to 75.5 yr. The plots are reproduced directly from the original publications. Note the significant departure from a log-linear relationship.

that the magnitude range or increment of the characteristic earthquake is about one-half magnitude unit, and that the increment between the minimum characteristic magnitude and the portion of the recurrence curve showing exponential behavior at recurrence rates greater than the rate for characteristic events is about one magnitude unit (Figure 9). In other words, the magnitude range showing nonexponential behavior in a cumulative plot is about 1.5 magnitude units. This is in general agreement with the model proposed by Singh *et al.* (1983) whereby they

identified a gap, γ, between the main shock magnitude and the maximum magnitude in the aftershock plus background seismicity plus foreshock sequence. The parameter γ appears to have values of about 1.7 along the Mexican subduction zone (Singh *et al.*, 1983) and 1.4 along the Alaskan subduction zone (Utsu, 1971).

Slip rate constraints on characteristic earthquake recurrence relationships. To provide a slip rate constraint on earthquake recurrence using the characteristic earthquake model, a frequency density function for magnitude must be specified. Although few data have been compiled to provide well-developed constraints on the form of the density function, the seismicity data shown in Figure 9 and reports of similar recurrence relationships in other parts of the world provide a basis for constructing a generalized form shown in Figure 10. We believe this to be a reasonable form, at least for illustrating the application of the model to estimating earthquake recurrence and the impact of its use on hazard assessments.

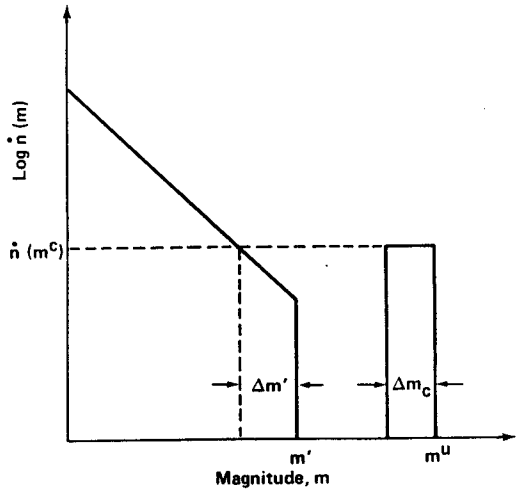

FIG. 10. Generalized frequency magnitude density function for the characteristic earthquake model. Magnitudes are exponentially distributed up to magnitude m'. The characteristic earthquake is uniformly distributed in the magnitude range of $m^u - \Delta m_c$ to m^u.

The model shown in Figure 10 consists of exponentially distributed magnitudes up to magnitude level m'. Above this magnitude lies the characteristic earthquake which is uniformly distributed in the magnitude range of $m^u - \Delta m_c$ to m^u at a rate density $\dot{n}(m^c)$. Using this density function, the slip rate constraint provided by equation (10) becomes

$$\mu A_f S = \frac{b(\dot{N}(m^0) - \dot{N}(m^c))\exp(-\beta(m' - m^0))M_0'}{(c-b)(1-\exp(-\beta(m'-m^0)))} + \frac{\dot{N}(m^c)M_0^u(1-10^{-c\Delta m_c})}{c\ln(10)\Delta m_c} \quad (15)$$

where $\dot{N}(m^c)$ is the cmulative rate of characteristic earthquakes [$\dot{N}(m^c) = \dot{n}(m^c)\Delta m_c$] and $\dot{N}(m^0)$ again represents the cumulative recurrence rate for earthquakes of magnitude greater than m^0. To use equation (15), five of the six parameters $\dot{N}(m^0)$, b, m', m^u, Δm_c, and $\dot{N}(m^c)$, must be specified along with the slip rate requiring a substantial amount of information in order to make assessments. To

apply the model to the common situation where the only parameters that can be estimated are S, b, and m^u, some simplifying assumptions must be made. For this analysis, we make the following assumptions: (1) Δm_c equals $\frac{1}{2}$ magnitude unit; (2) $m' = m^u - \Delta m_c$, as there is no reason to exclude the occurrence of any size event below m^u; and (3) $\dot{n}(m^c) \approx \dot{n}(m' - 1)$, which produces the desired flat portion in the cumulative curve. These assumptions appear to be reasonable first approximation given the data in Figure 9. We are currently analyzing the seismicity data in the region shown in Figure 9 and in other regions to further refine the density function. Applying these assumptions to equation (15) yields

$$\mu A_f S = \frac{(\dot{N}(m^0) - \dot{N}(m^c))\exp(-\beta(m^u - m^0 - 1/2))M_0{}^u}{(1 - \exp(-\beta(m^u - m^0 - 1/2)))} \cdot \left[\frac{b10^{-c/2}}{c - b} + \frac{b\exp(\beta)(1 - 10^{-c/2})}{c}\right] \quad (16)$$

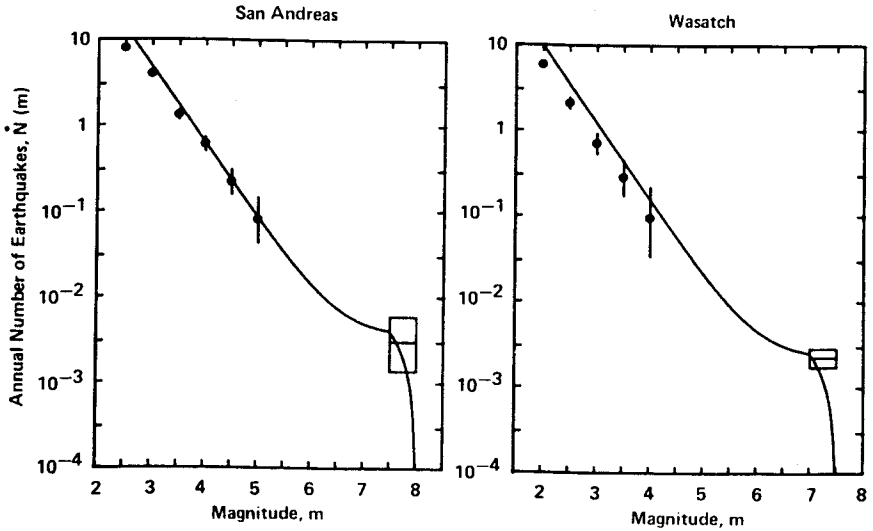

FIG. 11. Comparison of recurrence relationships based on the model presented in Figure 12 with historical seismicity and paleoseismicity data. Seismicity data, paleoseismicity data (shown by the boxes), and slip rates for the south-central segment of the San Andreas fault and the Wasatch fault are from Schwartz and Coppersmith (1984). The height of the boxes and the length of the bars through the data points represent one standard deviation error bars.

with

$$\dot{N}(m^c) = \frac{b\ \ln(10)(\dot{N}(m^0) - \dot{N}(m^c))\exp(-\beta(m^u - m^0 - 3/2))}{2(1 - \exp(-\beta(m^u - m^0 - 1/2)))}. \quad (17)$$

The term $[\dot{N}(m^0) - \dot{N}(m^c)]$ represents the rate of noncharacteristic, exponentially distributed earthquakes on the fault.

To test the reasonableness of the simplified characteristic earthquake model, recurrence rate estimates were developed using equation (16) for the south-central segment of the San Andreas fault and the Wasatch fault zone. These estimated rates are compared with the historical and paleoseismicity data for these fault zones

(discussed in detail in Schwartz and Coppersmith, 1984) in Figure 11. The solid circles represent the mean rates obtained from historical seismicity with their associated error bars. The boxes represent the mean rates for characteristic earthquakes obtained from geologic data with associated error bars. The width of the box represents the range in magnitude estimated for the characteristic events that have occurred on the faults. As can be seen, the estimated recurrence rates compare very well with the observed rates.

Implications of characteristic earthquake recurrence relationships to hazard assessments. Figure 12 compares the earthquake recurrence relationships for a single fault developed using an exponential magnitude distribution [equation (14)] with that developed using the characteristic magnitude distribution. Both relationships were developed using the same upper bound magnitude, b-value (for the exponential distribution magnitude range), and fault slip rate. The use of the characteristic

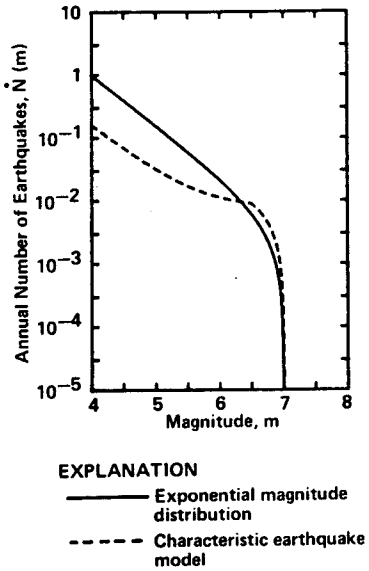

FIG. 12. Comparison of recurrence relationships based on an exponential magnitude distribution and characteristic earthquake distribution. Both relationships assume the same upper bound magnitude of b-value of 0.8, and fault slip rate.

earthquake model results in a slight increase in the frequency of the largest events and a decrease in the frequency of the small-to-moderate events from that obtained using an exponential magnitude distribution.

The hazard curves computed for the three sites in Figure 1 using these two recurrence relationships are compared in Figure 13. At close distances to the fault, use of the characteristic earthquake model results in lower hazard levels due to the lower rate of the small-to-moderate earthquakes, which contribute the most to the hazard at close distances. At greater distances and larger acceleration levels, where the contributions from larger magnitude events dominate the computed hazard, the characteristic earthquake model tends to produce higher hazard levels than the exponential model.

It should be noted that one form of truncation of the exponential distribution currently in use, namely direct truncation of the complementary cumulative rela-

tionship at m^u, produces a somewhat similar effect on computed hazard as the characteristic earthquake model. However, this results simply from the discretization of the truncated cumulative recurrence curve, rather than a direct choice of a greater frequency for events in the highest magnitude increment such as the model shown in Figure 10.

Use of the characteristic model constrained by slip rate produces similar sensitivity in hazard estimates to changes in slip rate, upper bound magnitude as those obtained for the exponential distribution constrained by slip rate. As indicated by equations (16) and (17), the recurrence rates $\dot{N}(m^0)$ and $\dot{N}(m^c)$ are directly proportional to slip rate and thus by equation (14), the computed hazard is directly proportional to the slip rate.

The effect of changes in upper bound magnitude and b-value on the recurrence relationship is shown in Figure 14. Changes in the upper bound magnitude have a somewhat greater effect on the recurrence rate for smaller magnitudes when the

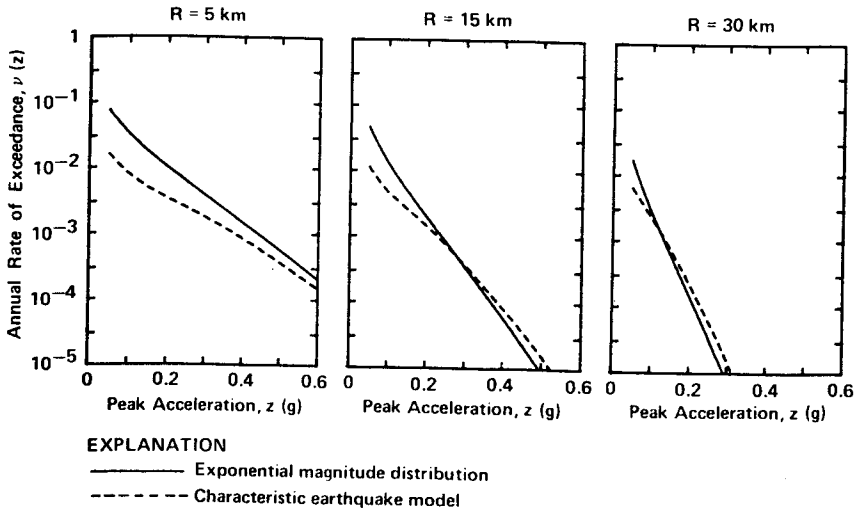

FIG. 13. Comparison of computed hazard (peak acceleration) from the exponential magnitude distribution and the characteristic earthquake distribution ($b = 0.8$, $m^u = 7$).

characteristic magnitude distribution is used then the effect shown in Figure 2 for the exponential magnitude distribution. This is due to the greater concentration of seismic moment release near the upper bound magnitude for the characteristic model as opposed to the exponential model. For the same reason, changes in b-value have a smaller effect on the recurrence relationships for a characteristic model than for an exponential model (see Figure 5).

The effects on hazard at the three sites in Figure 1 of changes in upper bound magnitude and b-value in the characteristic earthquake model with slip rate constraints are shown in Figure 15. The results are consistent with the effects on the recurrence relationships shown in Figure 14 and show a greater sensitivity to changes in upper bound magnitude than observed for the exponential magnitude distributions (Figure 3) and lower sensitivity to b-value than the exponential magnitude distribution (Figure 6).

EFFECT OF ATTENUATION RELATIONSHIP

The hazard curve comparisons presented in the previous sections were made using an attenuation relationship appropriate for the Western United States. The main characteristics of the selected attenuation relationship (Sadigh, 1983) are a reduced dependence on magnitude in the near-field and a large change in slope with respect to log R over the distance range of 1 to 30 km. To test the sensitivity of the above comparisons to the choice of attenuation relationships, the parametric analyses were repeated using an attenuation relationship recently developed for eastern Canada by Atkinson (1984). Atkinson's relationship has a strong magnitude dependence in the near-field (magnitude independent shape) and shows only small changes in slope for distances greater than 10 km. The results of these analyses are summarized in Figure 16.

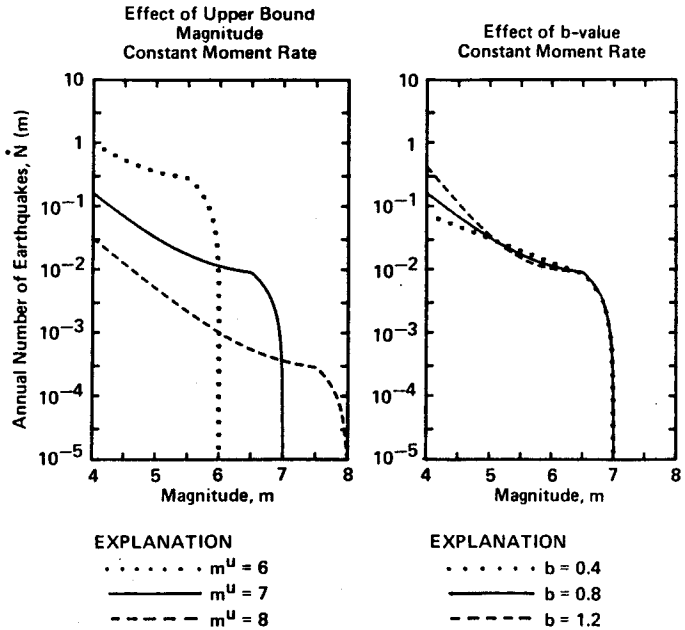

FIG. 14. Effects on slip rate constrained recurrence relationships of variations in upper bound magnitude and b-value, assuming a characteristic earthquake model.

Shown in the figure are the effects of changing the upper bound magnitude, the b-value, and the form of the magnitude distribution in the slip rate constrained recurrence relationships on the computed hazard as a function of distance for three acceleration levels. On the left are the results obtained using Sadigh's (1983) attenuation relationship and on the right are the results obtained using Atkinson's (1984) attenuation relationship. As can be seen, both attenuation relationships yield similar results except that the curves obtained using Atkinson's relationship are shifted to greater distances, reflecting the lower rate of attenuation in eastern Canada compared to California. Thus, one would expect to see similar sensitivity of computed hazard levels to changes in the recurrence relationship parameters, regardless of the applicable attenuation relationship.

DISCUSSION

The use of geologic slip rate to constrain estimates of earthquake recurrence, and ultimately seismic hazards, is based on some fundamental underlying assumptions, including: (1) the slip rate is an indicator of the average rate of seismic energy release; and (2) the long-term average past behavior is representative of the short-term future behavior (e.g., next 50 yr). The validity of the latter assumption cannot be directly assessed, but we can compare the long-term (geologic) average past

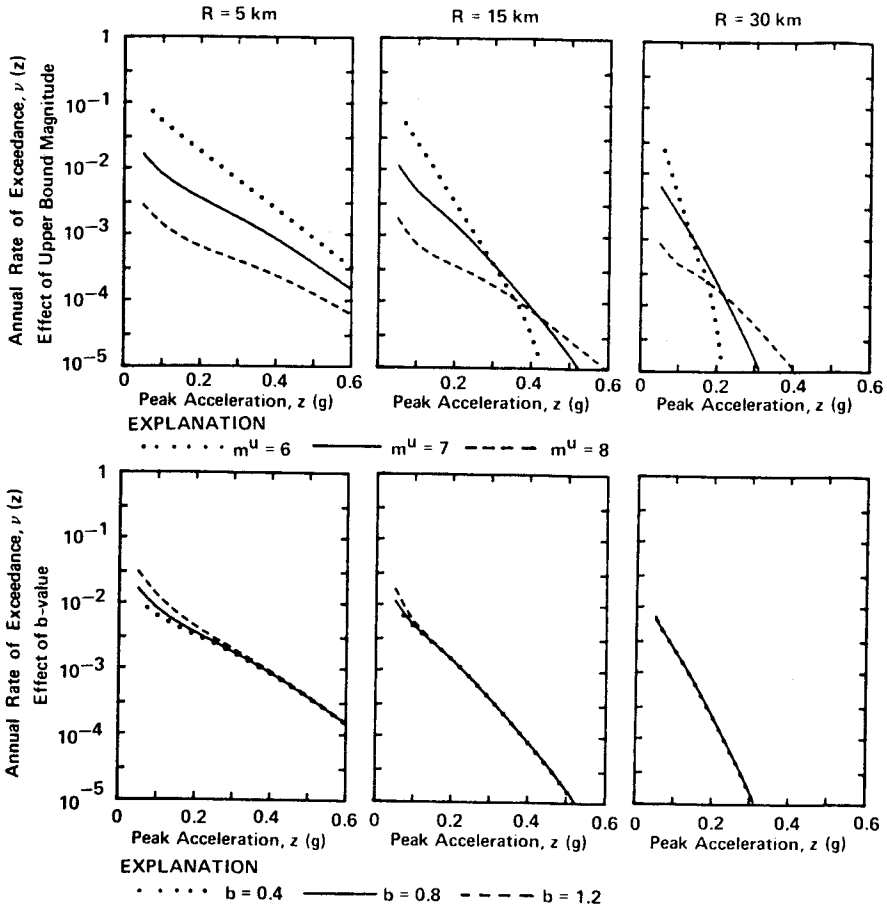

FIG. 15. Effect on computed hazard (peak acceleration) of variations in upper bound magnitude and *b*-value, assuming a characteristic earthquake model.

behavior to the short-term (historical) past behavior. In some cases, we can also compare the long-term average slip rate with geologic evidence for the recurrence of paleoseismic events. Tests of the validity of either assumption based on comparisons of slip rate and seismicity data cannot usually be made for individual faults because of the relatively short record of historical seismicity. For those cases where the historical record contains several large-magnitude earthquakes on an individual

fault, the geologic slip rate is usually in agreement with the seismic slip rate. The San Jacinto fault is one example (Thatcher *et al.*, 1975; Anderson, 1979).

For the majority of cases where paleoseismic data are not available or the historical record is too short to characterize the recurrence behavior of individual faults, we may substitute space for time by looking at large regions and compare activity rates based on geologic slip rates with those based on seismicity data.

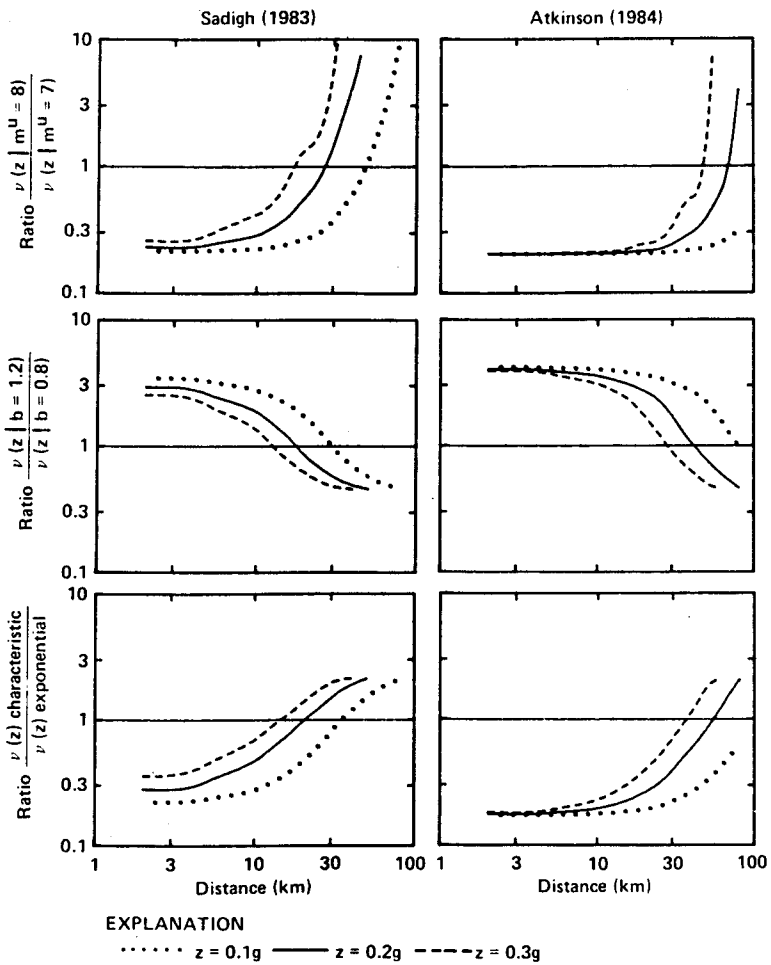

FIG. 16. Effect of attenuation relationship on sensitivity of hazard to changes in m^u (*top row*), *b*-value (*middle row*), and form of magnitude distribution (*bottom row*) when using slip rate constraints on the recurrence relationship ($m^u = 7$, $b = 0.8$, and exponential distribution unless otherwise indicated).

Unfortunately, in doing so we are forced to include several faults, and we lose the resolving power regarding fault-specific recurrence behavior. However, a regional analysis does provide some constraints on whether fault-specific recurrence models result in activity rates that are reasonably consistent with the observational seismicity record, which is the only independent data set available.

This section of the paper shows how slip rate recurrence on actual faults compares

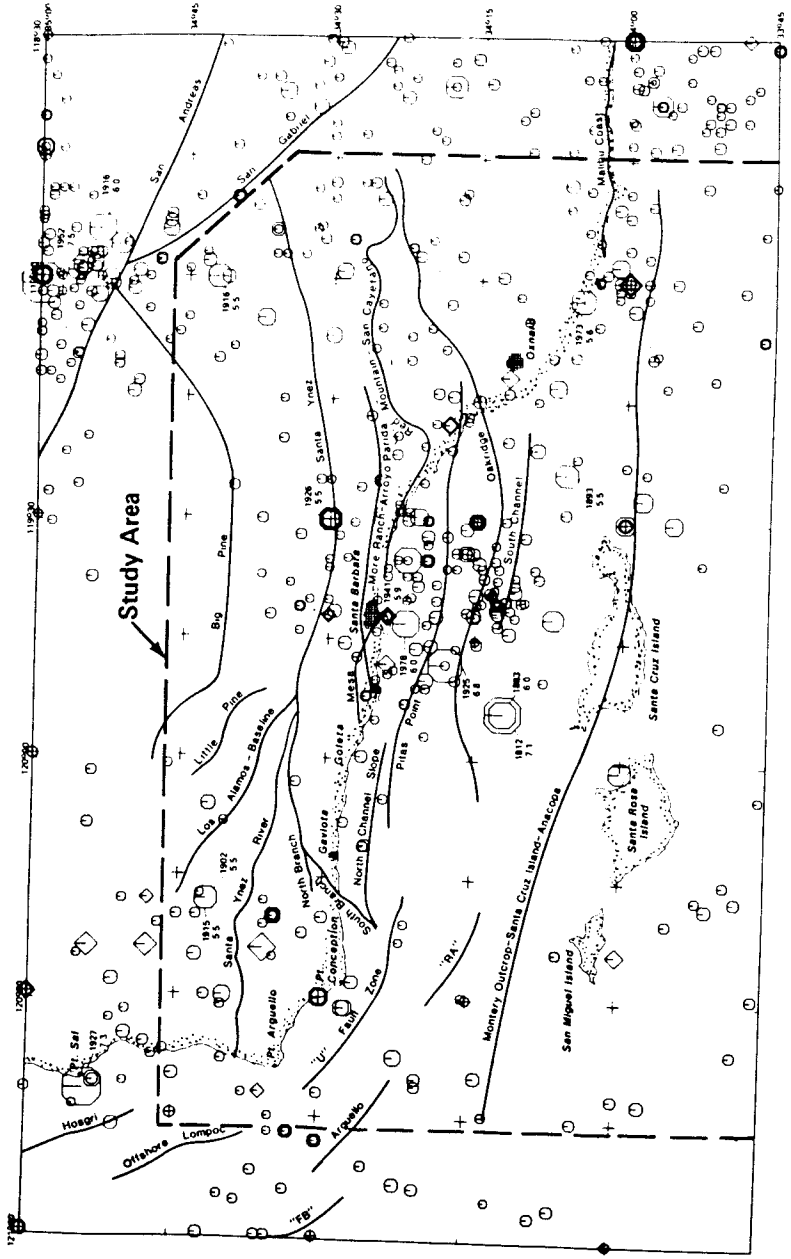

FIG. 17. Map of the western Transverse Ranges showing historical earthquake epicenters and identified active faults.

regional recurrence based on seismicity data and the effect of the exponential and characteristic recurrence models on that comparison.

Figure 17 shows a map of the western Transverse Ranges and the Santa Barbara Channel region of Southern California. The map shows the distribution of recorded seismicity (open circles) and mapped larger Quaternary faults in the region. A comparison (shown in Figure 18) was made using both the exponential magnitude distribution [equation (11)] and the characteristic earthquake magnitude distribution [equations (16) and (17)]. The regional b-value for the study area outlined in Figure 17 was computed to be 0.75 using Weichert's (1980) maximum likelihood formulation. The recurrence estimates based on historical seismicity are shown by the dots in Figure 18 with their associated error bars. For the 15 faults located

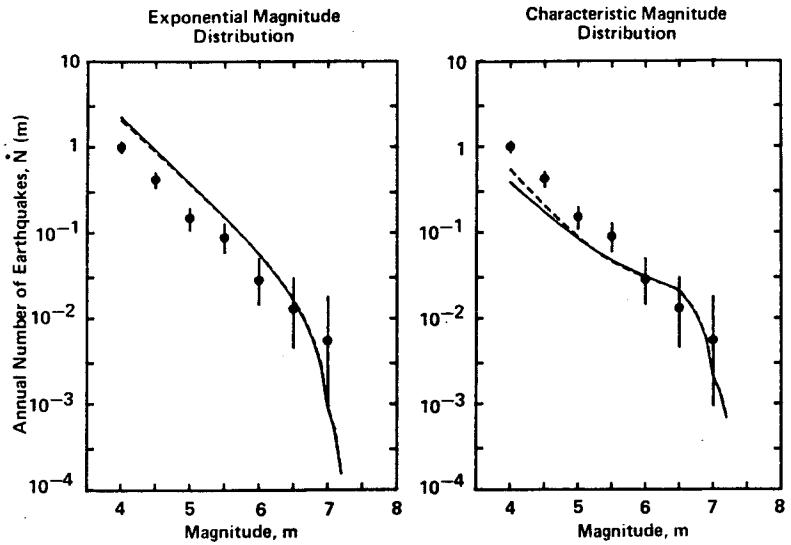

FIG. 18. Comparison of recurrence relationships based on slip rate and historical seismicity. The region is that shown in Figure 17. Seismicity data are shown by the points, and bars represent one standard deviation on estimates of the cumulative recurrence rate at each magnitude increment. The *left plot* is based on an assumed exponential magnitude distribution for each fault in the region. The *right plot* is based on a characteristic earthquake model. The solid curve assumes the b-value on individual faults is the same as the regional b-value. The dashed curve assumes that the b-values of individual faults can be adjusted such that all of the faults in combination match the regional b-value.

completely or partially in the study area, there is varying degrees of uncertainty in the slip rate, fault geometry, and upper bound magnitude. This uncertainty was incorporated probabilistically in the recurrence estimates using the techniques described by Kulkarni *et al.* (1984).

The solid curves in Figure 18 show the computed mean recurrence estimates using the fault slip rates. As can be seen, both forms of the magnitude distribution yield reasonable estimates of the recurrence for the larger earthquakes, indicating that the observed seismic moment release in the region is consistent with the observed average rate of crustal deformation represented by fault slip rates.

The comparisons in Figure 18 show that the match between the predicted seismicity rate and the observed seismicity rate is poorest for the small magnitude

earthquakes. The exponential distribution model overpredicts the rate of magnitude 4 to 5 earthquakes by about a factor of 2, and the characteristic earthquake model underpredicts the rate for these events by about a factor of 2. Part of this discrepancy results from the fact that when a regional recurrence rate is computed by summing the contributions from individual faults that all have the same b-value but have different upper bound magnitudes, the resulting regional b-value is somewhat different than the value used for each of the faults. For the exponential model, the computed b-value for the recurrence estimated given by the solid curve is 0.77. By reducing the b-value for the individual faults, a regional b-value of 0.75 is recovered, shown by the dashed line. For the characteristic earthquake model, the resulting b-value (assuming the regional recurrence is exponentially distributed) is 0.61. By increasing the b-value on the individual faults to 0.90, a regional b-value of 0.75 is obtained, again shown by the dashed curve.

The results shown in Figure 18 indicate that even after correcting to produce the correct regional b-value, both recurrence models produce significant differences in the rate of smaller earthquakes as compared to the observed historical rate. There are several explanations for these differences. If one accepts the characteristic earthquake model as a more correct representation of the recurrence for individual faults, then, from the results shown in Figure 12, use of the exponential distribution model would overpredict the recurrence rate for smaller earthquakes on an individual fault, and by extension, overpredict the regional rate for smaller events. The underprediction of the regional rate for smaller events by the characteristic earthquake model may result from the fact that only the slip rate on the larger regional faults were included in the analysis. It is likely that part of the smaller magnitude seismicity observed historically in the region occurred on smaller faults, many of which may not as yet have been identified.

The implications of the comparisons shown in Figure 18 to hazard assessments are very dependent upon the particular engineering problem being analyzed. If the analysis is being done for a structure that is primarily sensitive to longer period ground motions produced by the larger earthquakes or if low probabilities of exceedance ($<10^{-3}$) are being considered, then both recurrence models would yield similar results. For sites near the identified major faults, use of the exponential magnitude distribution would tend to yield conservative estimates of the probabilities of exceeding various levels of peak ground acceleration especially at high probabilities of exceedance ($>10^{-2}$). Perhaps a realistic representation of the distribution of seismicity in a region for hazard assessment would be to use the characteristic earthquake model to represent the recurrence of earthquakes on the major faults and to include an areal source (source zone) to model additional small-magnitude seismicity occurring on smaller, unidentified, faults. The choice of the "best" representation should be evaluated on a case by case basis in terms of the application of the computed hazard levels.

Acknowledgments

The authors are grateful to C. Allin Cornell for his constructive review of this manuscript. Many thanks also to Dennis Fischer for preparation of the graphics.

References

Aki, K. (1966). Generation and propagation of G-waves from the Niigata earthquake of June 19, 1964. 2. Estimation of earthquake movement, released energy, and stress-strain drop from G-wave spectrum, *Bull. Earthquake Res. Inst., Tokyo Univ.* **44,** 23–88.

...K. (1984). Asperities, barriers, characteristic earthquakes and strong motion prediction, *J. Geophys. Res.* **89,** 5, 867–5, 872.

Anderson, J. G. (1979). Estimating the seismicity from geological structure for seismic-risk studies, *Bull. Seism. Soc. Am.* **69,** 135–158.

Anderson, J. G. and J. E. Luco (1983). Consequences of slip rate constraints on earthquake recurrence relations, *Bull. Seism. Soc. Am.* **73,** 471–496.

Atkinson, G. M. (1984). Attenuation of strong ground motions in Canada from a random vibration approach, *Bull. Seism. Soc. Am.* **74,** 2629–2653.

Bakun, W. H. and T. V. McEvilly (1984). Recurrence models and Parkfield, California, earthquakes, *J. Geophys. Res.* **89,** 3051–3058.

...nder, B. (1983). Maximum likelihood estimation of b-values for magnitude grouped data, *Bull. Seism. Soc. Am.* **53,** 831–852.

Båth, M. (1981). Earthquake recurrence of a particular type, *Pure Appl. Geophys.* **119,** 1063–1076.

Båth, M. (1982). Seismic energy mapping applied to Sweden, *Tectonophysics* **81,** 85–98.

Båth, M. (1983). Earthquake frequency and energy in Greece, *Tectonophysics* **95,** 233–252.

Berrill, J. B. and R. D. Davis (1980). Maximum entropy and the magnitude distribution, *Bull. Seism. Soc. Am.* **70,** 1823–1831.

Brune, J. N. (1968). Seismic moment, seismicity and rate of slip along major fault zones, *J. Geophys. Res.* **73,** 777–784.

Campbell, K. W. (1977). The use of seismotectonics in the Bayesian estimation of seismic risk, Report No. UCLA-ENG-7744, School of Engineering and Applied Sciences, University of California, Los Angeles, California.

Campbell, K. W. (1981). Near-source attenuation of peak horizontal acceleration, *Bull. Seism. Soc. Am.* **71,** 2039–2070.

Caputo, M. (1977). A mechanical model for the statistics of earthquakes, magnitude, moment, and fault distribution, *Bull. Seism. Soc. Am.* **67,** 849–861.

Cornell, C. A. (1968). Engineering seismic risk analysis, *Bull. Seism. Soc. Am.* **58,** 1583–1606.

Cornell, C. A. and E. H. Van Marke (1969). The major influences on seismic risk, Proceedings Third World Conference on Earthquake Engineering, Santiago, Chile, A-1, 69–93.

Davison, F. C. and C. H. Scholz (1984). Test of the characteristic earthquake model for the Aleutian Arc (abstract), *EOS* **65,** 242.

Doser, D. I. and R. B. Smith (1982). Seismic moment rates in the Utah region, *Bull. Seism. Soc. Am.* **72,** 525–555.

Gutenberg, B. and C. F. Richter (1954). *Seismicity of the Earth and Associated Phenomena*, Princeton University Press, Princeton, New Jersey.

Hanks, T. C. and H. Kanamori (1979). A moment magnitude scale, *J. Geophys. Res.* **84,** 2348–2350.

Joyner, W. B. and D. M. Boore (1981). Peak horizontal acceleration and velocity from strong-motion records including records from the 1979 Imperial Valley, California, Earthquake, *Bull. Seism. Soc. Am.* **71,** 2011–2038.

Kulkarni, R. B., R. R. Youngs, and K. J. Coppersmith (1984). Assessment of confidence intervals for results of seismic hazard analysis, *Proceedings of the Eighth World Conference on Earthquake Engineering* **1,** 263–270.

Lahr, J. C. and C. D. Stephens (1982). Alaska seismic zone: possible example of nonlinear magnitude distribution for faults, *Earthquake Notes* **53,** 66.

Main, I. G. and P. W. Burton (1981). Rates of crustal deformation inferred from seismic moment and Gumbel's third distribution of extreme magnitude values, in *Earthquakes and Earthquake Engineering—Eastern United States*, J. E. Beavers, Editor, Ann Arbor Science Publishers, Inc., Ann Arbor, Michigan.

Main, I. G. and P. W. Burton (1984). Physical links between crustal deformation, seismic movement, and seismic hazard for regions of varying seismicity, *Geophys. J. R. Astr. Soc.* **79,** 469–488.

Merz, H. A. and C. A. Cornell (1973). Seismic risk analysis based on a quadratic magnitude-frequency law, *Bull. Seism. Soc. Am.* **63,** 1999–2006.

Molnar, P. (1979). Earthquake recurrence intervals and plate tectonics, *Bull. Seism. Soc. Am.* **69,** 115–133.

Papastamatiou, D. (1980). Incorporation of crustal deformation to seismic hazard analysis, *Bull. Seism. Soc. Am.* **70,** 1321–1335.

Purcaru, G. (1975). A new magnitude-frequency relation for earthquakes and a classification of relation types, *Geophys. J. R. Astr. Soc.* **42,** 67–69.

Richter, C. F. (1958). *Elementary Seismology*, W. H. Freeman and Company, San Francisco, California.

Sadigh, K. (1983). Considerations in the Development of Site-Specific Spectra, Proceedings USGS/US

NRC Workshop on Site-Specific Effects of Soil and Rock on Ground Motion and the Implications for Earthquake-Resistant Design, Santa Fe, New Mexico, July 26–28, *U.S. Geol. Surv., Open-File Rept. 83-845*, 423–458.

Schlien, S. and M. N. Toksoz (1970). Frequency-magnitude statistics of earthquake occurrence, *Earthquake Notes* **41**, 5–18.

Schwartz, D. P. and K. J. Coppersmith (1984). Fault behavior and characteristic earthquakes: examples from the Wasatch and San Andreas faults, *J. Geophys. Res.* **89**, 5681–5698.

Schwartz, D. P., K. J. Coppersmith, and F. H. Swan, III (1984). Methods for estimating maximum earthquake magnitude, *Eighth World Conference on Earthquake Engineering Proceedings* **1**, 279–286.

Sieh, K. E. (1978). Prehistoric large earthquakes produced by slip on the San Andreas fault at Pallett Creek, California, *J. Geophys. Res.* **83**, 3907–3939.

Sieh, K. E. (1984). Lateral offset and revised dates of large earthquakes at Pallett Creek, southern California, *J. Geophys. Res.* **89**, 7641–7670.

Singh, S. K., L. Astiz, and H. Havskov (1981). Seismic gaps and recurrence periods of large earthquakes along the Mexican subduction zone: a reexamination, *Bull. Seism. Soc. Am.* **71**, 827–843.

Singh, S. K., M. Rodriquez, and L. Esteva (1983). Statistics of small earthquakes and frequency of large earthquakes along the Mexico subduction zone, *Bull. Seism. Soc. Am.* **73**, 1779–1796.

Slemmons, D. B. (1977). State-of-the-art for assessing earthquake hazards in the United States, Report 6: faults and earthquake magnitude, U. S. Army Corps of Engineers, Waterways Experiment Station, Soils and Pavements Laboratory, Vicksburg, Mississippi, Miscellaneous Paper S-73-1, 129 pp.

Slemmons, D. B. (1982). Determination of design earthquake magnitudes for microzonation, *Proceedings of Third International Earthquake Microzonation Conference* **1**, 119–130.

Smith, S. W. (1976). Determination of maximum earthquake magnitude, *Geophys. Res. Letters* **3**, 351–354.

Swan, F. H., III, D. P. Schwartz, and L. S. Cluff (1980). Recurrence of moderate to large magnitude earthquakes produced by surface faulting on the Wasatch Fault zone, Utah, *Bull. Seism. Soc. Am.* **70**, 1431–1462.

Thatcher, W., J. A. Hileman, and T. C. Hanks (1975). Seismic slip distribution along the San Jacinto fault zone, southern California, and its implications, *Geol. Soc. Am. Bull.* **86**, 1140–1146.

Utsu, T. (1971). Aftershocks and earthquake statistics (III), *J. Fac. Sci. Hokkaido Univ. Ser. VII (Geophys.)* **3**, 379–441.

Wallace, R. E. (1970). Earthquake recurrence intervals on the San Andreas fault, *Geol. Soc. Am. Bull.* **81**, 2875–2890.

Weichert, D. H. (1980). Estimation of the earthquake recurrence parameters for unequal observation periods for different magnitudes, *Bull. Seism. Soc. Am.* **70**, 1337–1346.

Wesnousky, S. G., C. H. Scholz, K. Shimazaki, and T. Matsuda (1983). Earthquake frequency distribution and the mechanics of faulting, *J. Geophys. Res.* **88**, 9331–9340.

Yegulalp, T. M. and J. T. Kuo (1974) Statistical prediction of the occurrence of maximum magnitude earthquakes, *Bull. Seism. Soc. Am.* **64**, 393–414.

GEOMATRIX CONSULTANTS
ONE MARKET PLAZA
SPEAR STREET TOWER, SUITE 717
SAN FRANCISCO, CALIFORNIA 94105

Manuscript received 14 December 1984

Bulletin of the Seismological Society of America, Vol. 75, No. 4, pp. 965–1004, August 1985

TELESEISMIC TIME FUNCTIONS FOR LARGE, SHALLOW SUBDUCTION ZONE EARTHQUAKES

BY STEPHEN H. HARTZELL AND THOMAS H. HEATON

ABSTRACT

Broadband vertical *P*-wave records are analyzed from 63 of the largest shallow subduction zone earthquakes which have occurred in the circum-Pacific in the last 45 yr. Most of the records studied come from a common instrument, the Pasadena, California, Benioff 1–90 seismometer. Propagation and instrument effects are deconvolved from the *P*-wave records using a damped least-squares inversion to obtain the teleseismic source time function. The inversion has the additional constraint that the time function be positive everywhere. The period band over which the time functions are considered reliable is from 2.5 to 50 sec. Fourier displacement amplitude spectra computed for each of the 1–90 *P*-wave trains indicate spectral slopes measured between 2 and 50 sec of $\omega^{-1.0}$ to $\omega^{-2.25}$ with an average value of $\omega^{-1.5}$. These values assume an average attenuation of $t^* = 1.0$. The seismic moments derived from the *P*-wave time functions compare well with other published values for earthquakes having moments smaller than 2.5×10^{28} dyne-cm ($M_w = 8.2$). Because the 1–90 seismometer has little response at very long periods, this technique underestimates the moments of the very largest events. The time functions are characterized using five parameters: (1) spectral slope between 2 and 50 sec; (2) roughness of the time function; (3) multiplicity of sources; (4) pulse widths of individual sources; and (5) overall signal duration. The 63 earthquakes studied come from 15 subduction zones with a wide range in the ages of subducted lithosphere, convergence rates, and maximum size of earthquakes. Comparing the time function parameters with age, rate, and M_w of the subduction zone does not yield obvious global trends. However, most of the subduction zones do behave characteristically and can be grouped accordingly.

INTRODUCTION

In terms of the details of fault rupture or source complexity, our knowledge of the very largest earthquakes is limited. Until very recently, most of what was known about major earthquakes consisted of estimates of their focal mechanism and moment. Although this information is of fundamental interest, it is desirable to know more about the spatial and temporal distribution of moment release. The very largest earthquakes have been shallow thrust events at convergent plate boundaries. In this paper, we present the results of a survey study of teleseismic source time functions for major shallow thrust earthquakes. Sixty-three of the largest shallow subduction zone earthquakes that have occurred in the circum-Pacific in the last 45 yr are studied. Earthquakes from 15 different subduction zones with very different ages of subducted lithosphere and plate convergence rates are included.

The source complexity of the earthquakes is appraised by the physical features of the teleseismic source time functions. These features include the overall duration, multiple or single event character, individual source pulse widths, and roughness of the time function. The above measures of source size and complexity can then be compared with the age of subducted lithosphere, plate convergence rate, and other physical parameters of the subduction zone. Such comparisons are important for increasing our understanding of the worldwide distribution of the largest earth-